



# CHORUS

This is the accepted manuscript made available via CHORUS. The article has been published as:

## Pure negatively charged state of the NV center in n-type diamond

Yuki Doi, Takahiro Fukui, Hiromitsu Kato, Toshiharu Makino, Satoshi Yamasaki, Toshiyuki Tashima, Hiroki Morishita, Shinji Miwa, Fedor Jelezko, Yoshishige Suzuki, and Norikazu Mizuochi

Phys. Rev. B **93**, 081203 — Published 3 February 2016

DOI: [10.1103/PhysRevB.93.081203](https://doi.org/10.1103/PhysRevB.93.081203)

# Pure negatively charged state of the NV center in n-type diamond

Yuki Doi<sup>1</sup>, Takahiro Fukui<sup>1</sup>, Hiromitsu Kato<sup>2,3</sup>, Toshiharu Makino<sup>2,3</sup>, Satoshi Yamasaki<sup>2,3</sup>,  
Toshiyuki Tashima<sup>1</sup>, Hiroki Morishita<sup>1</sup>, Shinji Miwa<sup>1</sup>, Fedor Jelezko<sup>4</sup>, Yoshishige Suzuki<sup>1</sup>,  
and Norikazu Mizuochi<sup>1,3,a)</sup>

<sup>1</sup>*Graduate School of Engineering Science, Osaka University, Toyonaka, Osaka 560-8531, Japan*

<sup>2</sup>*Energy Technology Research Institute, National Institute of Advanced Industrial Science and  
Technology (AIST), Tsukuba, Ibaraki 305-8568, Japan*

<sup>3</sup>*CREST, Japan Science and Technology Agency, Kawaguchi, Saitama 332-0012, Japan*

<sup>4</sup>*Institut für Quantenoptik, Universität Ulm, Albert-Einstein-Allee 11, 89081 Ulm, Germany*

<sup>a)</sup> Electronic mail: mizuochi@mp.es.osaka-u.ac.jp

## Abstract

Optical illumination to negatively charged nitrogen-vacancy centers ( $NV^-$ ) inevitably causes stochastic charge-state transitions between  $NV^-$  and neutral charge state of the NV center. It limits the steady-state-population of  $NV^-$  to 5% at minimum ( $\sim 610$  nm) and 80% ( $\sim 532$  nm) at maximum in intrinsic diamond depending on the wavelength. Here, we show Fermi level control by phosphorus doping generates  $99.4 \pm 0.1\%$   $NV^-$  under 1  $\mu$ W and 593 nm excitation which is close to maximum absorption of  $NV^-$ . The pure  $NV^-$  shows a five-fold increase of luminescence and a four-fold enhancement of an optically detected magnetic resonance under 593 nm excitation compared with those in intrinsic diamond.

1 Nitrogen-vacancy (NV) centers in diamond are the most promising candidate for various  
2 applications such as quantum information science [1–8], magnetometry [9–13], and biosensing [14–  
3 16]. For these applications, controlling the charge state of the NV centers is crucial, because optical  
4 initialization and readout of the spin state of the NV centers are only possible in negatively charged  
5 one ( $NV^-$ ). However, upon illumination, the NV centers undergo stochastic charge-state transitions  
6 between  $NV^-$  and neutral charge state of the NV center ( $NV^0$ ) [17,18]. For example, upon excitation  
7 around 580 nm, where  $NV^-$  has the highest absorption [17,19],  $NV^-$  easily turns into the  $NV^0$  and the  
8 steady-state-population of  $NV^-$  decreases to about 10%, which could be revealed from single-shot  
9 charge-state measurements [17]. Therefore, illumination at 532 nm is usually used in the experiment  
10 of  $NV^-$ . This charge-state interconversion occurs upon illumination at any wavelength, so the steady-  
11 state  $NV^-$  population is always less than 75%–80% [17,20].

12 Generating a pure state including the charge state, close to 100%  $NV^-$  population, is very  
13 important for quantum information applications. Studies involving the pre-selection and reset of the  
14 charge state were carried out to achieve high-fidelity operation because of the instability of the  
15 charge states [1,4,5]. However, this approach makes scaling up of diamond quantum registers more  
16 challenging. Furthermore, single-shot readout of a nuclear spin indicates that the spin-flip probability  
17 of the conditional gate operation decreases because of the stochastic charge-state transitions [6,21].  
18 In addition, such charge-state transitions lead to spectral diffusion [18,22,23] of the zero-phonon line  
19 of  $NV^-$ , which reduces the efficiency of two-photon quantum interference [4]. For nanoscale sensing  
20 applications, it is crucial to keep  $NV^-$  stable near the surface for high spatial resolution [15];  
21 however,  $NV^-$  near the surface is unstable [24]. In addition, high-contrast fluorescence switching  
22 between pure bright  $NV^-$  and the pure dark state ( $NV^0$ ) is also very important for super-resolution  
23 microscopy [25].

24 Previously, NV charge states were controlled by heavy neutron irradiation [26], surface  
25 termination [27–29], and combined optical and electrical operations [30–33]. Most of them were

1 investigated by photoluminescence (PL) spectra, which only reveals a ratio of the charge states of the  
2 bright state. On the other hand, single-shot charge-state measurements can reveal the ratio of  $NV^-$   
3 and  $NV^0$  during illumination. Recently, deterministic control from  $NV^-$  to  $NV^0$  by a purely electrical  
4 operation was revealed from the single-shot charge-state measurements [34]. Doping with nitrogen is  
5 considered to be one way to control the  $NV^-$  population. Nitrogen donors (P1 centers) can donate  
6 electrons to  $NV^0$  in the dark region (without laser illumination), thereby changing its state to  $NV^-$ ,  
7 because the activation energy ( $E_A = 1.70$  eV) of P1 is less than the energy difference between the  
8 acceptor level, labeled  $(-/0)$ , of the NV center [35] and the conduction-band edge, as shown in Fig.  
9 1(a). Recently, charge states of ensemble NV centers were modulated by ion-implantation of  
10 phosphorus and boron atoms [36]. However, pure  $NV^-$  charge state, which can be revealed by the  
11 single-shot charge-state measurements, has not yet been realized in nitrogen doping and ion-  
12 implantation of phosphorus. Based on the activation energy, phosphorus doping during chemical  
13 vapor deposition (CVD) appears promising because that of phosphorus ( $E_A = 0.57$  eV) [37] is much  
14 less than that of P1. It should be noted that, so far, n-type conductivity in diamond has been only  
15 realized by the CVD synthesis technique. In the present study, we quantitatively investigate the  
16 charge-state population of NV centers by using single-shot readout measurements in slightly  
17 phosphorus-doped n-type diamond. We obtain a pure  $NV^-$  population ( $> 99\%$   $NV^-$ ) and report its  
18 dynamics.

19 Phosphorus-doped n-type diamond samples were epitaxially grown by CVD onto Ib-type (111)-  
20 oriented diamond substrates with phosphorus concentrations of  $5 \times 10^{16}$  atoms/cm<sup>3</sup> (sample A) and  
21 about  $5 \times 10^{15}$  atoms/cm<sup>3</sup> (sample B) [38]. A homebuilt confocal microscope system was used to  
22 optically address single NV centers [38]. All experiments were conducted at room temperature.

23 No color centers other than single NV centers were detected in our high-quality samples under  
24 visible illumination. Typically, a high incorporation of nitrogen (such as more than  $10^{15}$  atoms/cm<sup>3</sup>)  
25 during CVD growth generates many NV centers. It makes difficult to detect single NV centers. The

1 fact that we detect many single NV centers in our samples reflects an advantage of phosphorus  
2 doping. Figures 1(b) and 1(c) show PL raster scan images of n-type diamond (sample A) illuminated  
3 at 532 and 593 nm, respectively. Upon 532 nm illumination, the single NV center, labeled NV1,  
4 produces almost the same count rate ( $\sim 55$  kcounts/s) as does the NV center labeled NV2. Upon 593  
5 nm illumination, the counts rates of NV1 decreases because of the reduced  $NV^-$  population, as  
6 reported previously [17]. However, the counts rates from NV2 is about five times larger than that  
7 from NV1 (50 vs 10 kcounts/s). Moreover, in another area of samples A and B, more than ten single  
8 NV centers are bright under 593 nm illumination.

9 Weak excitation (typically  $1 \mu W$ ) at 593 nm wavelength makes the charge-state interconversion  
10 of NV center gently. Thereby this is used to real-time detection of the charge states [17]. The charge  
11 states are distinguished by photon counts with optical filters (we used a 650-nm longpass filter)  
12 which blocks the fluorescence of  $NV^0$ . From the real-time fluorescence trace of NV1, shown in Fig.  
13 2(a), the optically induced charge-state interconversion is recorded as telegraph signals of  
14 fluorescence from  $NV^-$  (high counts) and  $NV^0$  (low counts). In contrast to NV1, NV2 continuously  
15 keeps the fluorescence level of  $NV^-$  (Fig. 2(b)). These results suggest that NV2 populates to pure  
16  $NV^-$  under  $1 \mu W$ , 593 nm illumination.

17 In order to know charge-state population under 532 nm and 593 nm illumination, photon  
18 statistic measurements after illumination are performed. At NV1, average lifetimes of  $NV^0$  and  $NV^-$   
19 are 2.92 and 0.59 s, respectively, as determined by the hidden Markov model [17]. Therefore, for  
20 detection with  $1 \mu W$  illumination at 593 nm, if the detection time is sufficiently less than 0.59 s, we  
21 can nondestructively determine charge-states population from histogram of photon counts after  
22 arbitrarily initialization (single-shot charge-state measurement). Figures 3(a) and 3(b) are  
23 measurement sequences and histograms of photon counts of NV1 after initialization by  $30 \mu W$ , 532  
24 nm and  $1 \mu W$ , 593 nm illumination. For both initializations, the charge-state population of NV1 has  
25 a double Poisson distribution. For initialization at 532 nm, the charge-state populations are estimated

1 to be  $NV^0 : NV^- = 0.21 : 0.79$  from area of each peaks. Upon initialization at 593 nm,  $NV^-$  decreases  
2 to 0.12 on NV1 (Fig. 3(b)). These populations are almost the same as single NV centers in intrinsic  
3 diamond [17]. In contrast to NV1, NV2 has only one peak on the both sequences (Figs. 3(c) and  
4 3(d)). Peak widths and positions are quite similar to those of  $NV^-$  in Fig. 3(a). This result strongly  
5 suggests that detected photons in single-shot measurements come from pure  $NV^-$ . The difference in  
6 the  $NV^-$  population between NV1 and NV2 might be attributed to their different local environments  
7 (i.e., impurity and/or defects).

8 On the other hand, under 100  $\mu\text{W}$ , 532 nm illumination, the PL spectrum and the optically  
9 detected magnetic resonance (ODMR) intensity of  $NV^-$  on NV2 are the same as those of NV1 [38].  
10 These results suggest that, under 100  $\mu\text{W}$ , 532 nm illumination, the charge-state population of NV2  
11 is the same as that of NV1, despite a single peak being observed in Fig. 3(c). This fact implies that  
12 the charge state changes during the dark period (10 ms) between initialization and detection. To  
13 elucidate this fact, we average the PL intensity of NV2 after a time delay  $T_d$ . A 593 nm illumination  
14 with power of 230  $\mu\text{W}$  is used to observe decay of fluorescence. The measurement sequence and  
15 results are shown in Fig. 4(a). For  $T_d = 0.1$  ms, the PL intensity does not change during illumination.  
16 This means the charge state of NV2 is in a state of equilibrium during  $T_d$  and illumination. However,  
17 when  $T_d$  increases to 50 ms, increases of intensity and exponential decay of PL are observed. The  
18 increase of intensity can be attributed to the increase of the  $NV^-$  population during the dark period  
19 ( $T_d$ ). The subsequent decay is attributed to the decrease of the  $NV^-$  population during illumination by  
20 relatively higher power (230  $\mu\text{W}$ ) compared with 1  $\mu\text{W}$  in single-shot charge-state measurement.

21 To reveal the transition rate of the charge states during  $T_d$ , the PL intensity was measured as a  
22 function of  $T_d$  as shown in Fig. 4(b). The PL intensity clearly increases with  $T_d$  up to a saturation  
23 level. By fitting with a single exponential function, the transition rate from  $NV^0$  to  $NV^-$  during  $T_d$   
24 ( $\lambda_{\text{dark}}^0$ ) is estimated to  $1/(3.55 \pm 0.42 \text{ ms}) = 0.282 \pm 0.033 \text{ ms}^{-1}$ .

1 Next we investigate the dynamics during 593 nm illumination with several powers to show that  
2 the time constant for the charge-state transition is much longer than 30 ms under 1  $\mu\text{W}$ , which is the  
3 power of the charge detection in Figure 3. Figures 4(c) and 4(d) show the accumulated PL intensity  
4 of NV<sup>2</sup> under 100 and 1  $\mu\text{W}$ , 593 nm illumination after initialization by 532 nm laser. The time  
5 delay  $T_d$  between the 532 and 593 nm laser pulses was set to 10 ms, which is long enough for the  
6 NV<sup>-</sup> population to grow to more than 99%. At 100  $\mu\text{W}$ , 593 nm illumination, the PL intensity decays  
7 exponentially, as shown in Fig. 4(c). This result indicates that the rate from NV<sup>-</sup> to NV<sup>0</sup> by 593 nm  
8 illumination ( $\lambda_{593\text{nm}}^{0-}$ ) at 100  $\mu\text{W}$  is greater than  $\lambda_{\text{dark}}^{0-} + \lambda_{593\text{nm}}^{0-}$ , where  $\lambda_{593\text{nm}}^{0-}$  is a rate from NV<sup>0</sup> to  
9 NV<sup>-</sup> by 593 nm illumination. It was observed that the rate  $\lambda_{\text{dark}}^{0-} + \lambda_{593\text{nm}}^{0-}$  becomes smaller as the  
10 laser power decreases. At 1  $\mu\text{W}$  illumination, no decay in fluorescence intensity is observed, as  
11 shown in Fig. 4(d). This also supports charge-state is at equilibrium and purely populated to NV<sup>-</sup>  
12 under 1  $\mu\text{W}$ , 593 nm illumination.

13 We quantitatively estimate population of NV<sup>-</sup> to use transition rates. Under 593 nm cw  
14 illumination, the steady-state-population of NV<sup>-</sup> ( $p_{\text{NV}^-}$ ) can be calculated as follows [17,34]:

$$15 \quad p_{\text{NV}^-} = \frac{\lambda^{0-}}{\lambda^{0-} + \lambda^{0}} = \frac{\lambda_{593\text{nm}}^{0-} + \lambda_{\text{dark}}^{0-}}{\lambda_{593\text{nm}}^{0-} + \lambda_{\text{dark}}^{0-} + \lambda_{593\text{nm}}^{0}}. \quad (1)$$

16 We omitted  $\lambda_{\text{dark}}^{0-}$  because it is negligibly smaller than other rates (if it is not zero, histogram of Figs.  
17 2(c) and (d) must contain two Poisson distributions.). Here the optically induced transition rates  
18 ( $\lambda_{593\text{nm}}^{0-}$  and  $\lambda_{593\text{nm}}^{0}$ ) for NV1 under 1  $\mu\text{W}$ , 593 nm illumination can be obtained by average lifetimes  
19 of NV<sup>0</sup> and NV<sup>-</sup> in Fig. 2(a). These rates are estimated to be  $\lambda_{593\text{nm}}^{0-} = 1/2.92\text{s} = 0.342\text{s}^{-1}$  and  
20  $\lambda_{593\text{nm}}^{0} = 1/0.59\text{s} = 1.7\text{s}^{-1}$ . If these values of NV2 are assumed to be the same as those for NV1,  
21  $p_{\text{NV}^-}$  for NV2 under 1  $\mu\text{W}$ , 593 nm illumination is estimated to be  $p_{\text{NV}^-} = 0.994 \pm 0.001$  from

1 equation (1). For reference,  $p_{\text{NV}^-}$  for NV1 is calculated to be 0.170 (where  $\lambda_{\text{dark}}^{0-} = 0$ ), which is  
2 consistent with the charge-state population in Fig. 3(b). The case for the 532 nm excitation can be  
3 analyzed and it is indicated that a population consisting solely of the  $\text{NV}^-$  charge state can be  
4 generated by low-power 532 nm illumination [38].

5 In NV2, we found a four-fold enhancement of an ODMR under 593 nm excitation compared  
6 with that of NV1. Figure 4(e) shows ODMR spectra of NV1 and NV2 with a 1 mT magnetic field  
7 along the [111] direction of the diamond crystal under 200  $\mu\text{W}$ , 593 nm illumination. From NV2, the  
8 ODMR signal intensity from  $\text{NV}^-$ , which is the normalized fluorescence intensity, is almost 4.18  
9 times larger than that from NV1. This result confirms that the  $\text{NV}^-$  population of NV2 is much larger  
10 than that of NV1 and single peaks in Figs. 3(c) and 3(d) are from the  $\text{NV}^-$  charge state. To measure  
11 the ODMR spectra, we increased the 593 nm laser power to 200  $\mu\text{W}$ . At 200  $\mu\text{W}$ , the charge state is  
12 not considered to be a purely negative state. Under 593 nm, 1  $\mu\text{W}$  illumination, the ratio of  $\text{NV}^-$   
13 population between NV2 and NV1 is calculated to be  $100\% / 12\% = 8.33$  from the results of Fig. 3  
14 (b) and 3 (d). The enhanced ratio of ODMR signal intensity (= 4.18) is smaller than it. The main  
15 reason is considered to be due to the smaller ratio of  $\text{NV}^-$  population at the high laser power (200  
16  $\mu\text{W}$ ). In our case, NV1 and NV2 are aligned to [111] direction of diamond crystal. Therefore, we  
17 assume the microwave power, the amplitude and the polarization of laser of NV2 are the same with  
18 those of NV1. In the general case that NVs feels different microwave power, amplitude and  
19 polarization of laser with each other, we need to consider the effects of broadening of the  
20 spectra [39].

21 Finally, we measured spin-coherence time  $T_2$  by Hahn echo technique, because a long  $T_2$  is  
22 critical for quantum information and sensing. As a result,  $T_2$  is estimated to be  $19.77 \pm 0.27 \mu\text{s}$  for  
23 NV2 in sample A ( $[\text{P}] = 5 \times 10^{16} \text{ atoms/cm}^3$ ) and  $49.6 \pm 2.2 \mu\text{s}$  for sample B ( $[\text{P}] = 5 \times 10^{15}$   
24  $\text{atoms/cm}^3$ ) [38]. Previously, dependence of nitrogen donors (i.e., P1 centers) concentration on  $T_2$  of  
25 P1 centers was investigated and  $T_2$  of P1 centers is estimated to be about 1 ms and 100  $\mu\text{s}$  for the P1



1 concentration of  $5 \times 10^{15}$  and  $5 \times 10^{16} \text{ cm}^{-3}$ , respectively [40]. We expect that the dependence of the  
2 phosphorus concentration on  $T_2$  of NV centers to be almost the same as that of the P1 center because  
3 the unpaired electrons localize on their atoms. However, the present results of  $T_2$  are shorter than the  
4 expected values. It can be attributed to other impurities or defects [41]. In other words, if these  
5 impurities or defects could be removed and if  $^{12}\text{C}$  could be enriched,  $T_2$  in n-type diamond should  
6 become comparable to the long (millisecond order)  $T_2$  of high-quality intrinsic  $^{12}\text{C}$ -enriched  
7 diamond [13,42].

8 In summary, we investigated the  $\text{NV}^-$  population and its dynamics in phosphorus-doped n-type  
9 diamond by using nondestructive, single-shot readout measurements of the NV charge state. In  
10 phosphorus-doped n-type diamond, the results reveal that the  $\text{NV}^-$  charge state that populates over  
11 99% of the NV centers is generated by  $1 \mu\text{W}$  illumination at 593 nm. Under these illumination  
12 conditions, we obtain an almost five-fold increase in luminescence and a four-fold increase in the  
13 ODMR signal compared with the corresponding results for NV centers in intrinsic diamond. By  
14 analyzing the  $\text{NV}^-$  population as a function of illumination, we show that this approach would  
15 increase the  $\text{NV}^-$  population not only under 593 nm illumination but also under illumination by other  
16 wavelengths, such as 532 nm. These results are expected to significantly enhance the versatile  
17 potential of NV centers.

18  
19 This work was supported by JSPS KAKENHI Grant Number 15J05801. The authors gratefully  
20 acknowledge the financial support from NICT, as well as from JST CREST program. FJ  
21 acknowledges DFG, EU, ERC, Volkswagenstiftung, and DARPA.

22  
23  
24

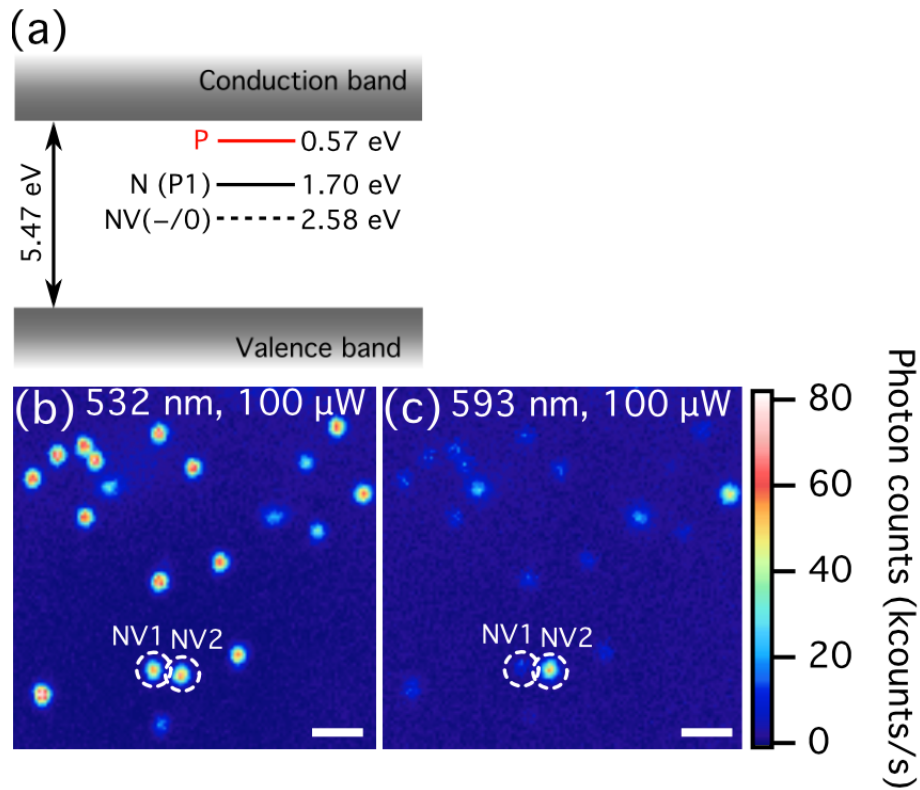
## 1 REFERENCES

- 2 [1] G. Waldherr, Y. Wang, S. Zaiser, M. Jamali, T. Schulte-Herbrüggen, H. Abe, T.  
3 Ohshima, J. Isoya, J. F. Du, P. Neumann, and J. Wrachtrup, *Nature (London)* **506**, 204  
4 (2014).
- 5 [2] P. C. Maurer, G. Kucsko, C. Latta, L. Jiang, N. Y. Yao, S. D. Bennett, F. Pastawski, D.  
6 Hunger, N. Chisholm, M. Markham, D. J. Twitchen, J. I. Cirac, and M. D. Lukin, *Room-*  
7 *temperature quantum bit memory exceeding one second.*, *Science* **336**, 1283 (2012).
- 8 [3] T. van der Sar, Z. H. Wang, M. S. Blok, H. Bernien, T. H. Taminiau, D. M. Toyli, D. A.  
9 Lidar, D. D. Awschalom, R. Hanson, and V. V. Dobrovitski, *Nature (London)* **484**, 82  
10 (2012).
- 11 [4] H. Bernien, B. Hensen, W. Pfaff, G. Koolstra, M. S. Blok, L. Robledo, T. H. Taminiau,  
12 M. Markham, D. J. Twitchen, L. Childress, and R. Hanson, *Nature (London)* **497**, 86  
13 (2013).
- 14 [5] L. Robledo, L. Childress, H. Bernien, B. Hensen, P. F. A. Alkemade, and R. Hanson,  
15 *Nature (London)* **477**, 574 (2011).
- 16 [6] P. Neumann, J. Beck, M. Steiner, F. Rempp, H. Fedder, P. R. Hemmer, J. Wrachtrup,  
17 and F. Jelezko, *Single-shot readout of a single nuclear spin*, *Science* **329**, 542 (2010).
- 18 [7] L. Childress, M. V. G. Dutt, J. M. Taylor, A. S. Zibrov, F. Jelezko, J. Wrachtrup, P. R.  
19 Hemmer, and M. D. Lukin, *Coherent dynamics of coupled electron and nuclear spin*  
20 *qubits in diamond.*, *Science* **314**, 281 (2006).
- 21 [8] V. Jacques, E. Wu, F. Grosshans, F. Treussart, P. Grangier, A. Aspect, and J.-F.  
22 Roch, *Experimental Realization of Wheeler's Delayed-Choice Gedanken Experiment*,  
23 *Science* **315**, 966 (2007).
- 24 [9] J. R. Maze, P. L. Stanwix, J. S. Hodges, S. Hong, J. M. Taylor, P. Cappellaro, L. Jiang,  
25 M. V. G. Dutt, E. Togan, A. S. Zibrov, A. Yacoby, R. L. Walsworth, and M. D. Lukin,  
26 *Nanoscale magnetic sensing with an individual electronic spin in diamond*, *Nature*  
27 *(London)* **455**, 644 (2008).
- 28 [10] G. Balasubramanian, I. Y. Chan, R. Kolesov, M. Al-Hmoud, J. Tisler, C. Shin, C. Kim,  
29 A. Wojcik, P. R. Hemmer, A. Krueger, T. Hanke, A. Leitenstorfer, R. Bratschitsch, F.  
30 Jelezko, and J. Wrachtrup, *Nature (London)* **455**, 648 (2008).
- 31 [11] H. J. Mamin, M. Kim, M. H. Sherwood, C. T. Rettner, K. Ohno, D. D. Awschalom, and  
32 D. Rugar, *Nanoscale Nuclear Magnetic Resonance with a Nitrogen-Vacancy Spin*  
33 *Sensor*, *Science* **339**, 557 (2013).
- 34 [12] F. Shi, X. Kong, P. Wang, F. Kong, N. Zhao, R.-B. Liu, and J. Du, *Sensing and atomic-*  
35 *scale structure analysis of single nuclear-spin clusters in diamond*, *Nat. Phys.* **10**, 21  
36 (2013).
- 37 [13] G. Balasubramanian, P. Neumann, D. J. Twitchen, M. Markham, R. Kolesov, N.  
38 Mizuochi, J. Isoya, J. Achard, J. Beck, J. Tisler, V. Jacques, P. R. Hemmer, F.  
39 Jelezko, and J. Wrachtrup, *Ultralong spin coherence time in isotopically engineered*  
40 *diamond.*, *Nat. Mater.* **8**, 383 (2009).
- 41 [14] L. P. McGuinness, Y. Yan, A. Stacey, D. A. Simpson, L. T. Hall, D. Maclaurin, S.  
42 Praver, P. Mulvaney, J. Wrachtrup, F. Caruso, R. E. Scholten, and L. C. L. Hollenberg,  
43 *Quantum measurement and orientation tracking of fluorescent nanodiamonds inside*  
44 *living cells*, *Nat. Nanotechnol.* **6**, 358 (2011).
- 45 [15] T. Staudacher, F. Shi, S. Pezzagna, J. Meijer, J. Du, C. A. Meriles, F. Reinhard, and J.  
46 Wrachtrup, *Nuclear Magnetic Resonance Spectroscopy on a (5-Nanometer)<sup>3</sup> Sample*  
47 *Volume*, *Science* **339**, 561 (2013).
- 48 [16] D. Le Sage, K. Arai, D. R. Glenn, S. J. DeVience, L. M. Pham, L. Rahn-Lee, M. D.  
49 Lukin, A. Yacoby, A. Komeili, and R. L. Walsworth, *Nature* **496**, 486 (2013).

- 1 [17] N. Aslam, G. Waldherr, P. Neumann, F. Jelezko, and J. Wrachtrup, *Photo-induced*  
2 *ionization dynamics of the nitrogen vacancy defect in diamond investigated by single-*  
3 *shot charge state detection*, New J. Phys. **15**, 013064 (2013).
- 4 [18] P. Siyushev, H. Pinto, M. Vörös, A. Gali, F. Jelezko, and J. Wrachtrup, *Optically*  
5 *Controlled Switching of the Charge State of a Single Nitrogen-Vacancy Center in*  
6 *Diamond at Cryogenic Temperatures*, Phys. Rev. Lett. **110**, 167402 (2013).
- 7 [19] A. S. Trifonov, J. C. Jaskula, C. Teulon, D. R. Glenn, N. Bar-Gill, and R. L. Walsworth,  
8 *Limits to Resolution of CW STED Microscopy*, Adv. At., Mol., Opt. Phys. **62**, 279  
9 (2013).
- 10 [20] X.-D. Chen, C.-L. Zou, F.-W. Sun, and G.-C. Guo, *Optical manipulation of the charge*  
11 *state of nitrogen-vacancy center in diamond*, Appl. Phys. Lett. **103**, 013112 (2013).
- 12 [21] G. Waldherr, J. Beck, M. Steiner, P. Neumann, A. Gali, T. Frauenheim, F. Jelezko, and  
13 J. Wrachtrup, *Dark states of single nitrogen-vacancy centers in diamond unraveled by*  
14 *single shot NMR.*, Phys. Rev. Lett. **106**, 157601 (2011).
- 15 [22] A. Stacey, D. A. Simpson, T. J. Karle, B. C. Gibson, V. M. Acosta, Z. Huang, K.-M. C.  
16 Fu, C. Santori, R. G. Beausoleil, L. P. McGuinness, K. Ganesan, S. Tomljenovic-  
17 Hanic, A. D. Greentree, and S. Prawer, *Near-surface spectrally stable nitrogen*  
18 *vacancy centres engineered in single crystal diamond.*, Adv. Mater. **24**, 3333 (2012).
- 19 [23] V. M. Acosta, C. Santori, A. Faraon, Z. Huang, K.-M. C. Fu, A. Stacey, D. A. Simpson,  
20 K. Ganesan, S. Tomljenovic-Hanic, A. D. Greentree, S. Prawer, and R. G. Beausoleil,  
21 *Dynamic Stabilization of the Optical Resonances of Single Nitrogen-Vacancy Centers*  
22 *in Diamond*, Phys. Rev. Lett. **108**, 206401 (2012).
- 23 [24] B. K. Ofori-Okai, S. Pezzagna, K. Chang, M. Loretz, R. Schirhagl, Y. Tao, B. A.  
24 Moores, K. Groot-Berning, J. Meijer, and C. L. Degen, *Spin properties of very shallow*  
25 *nitrogen vacancy defects in diamond*, Phys. Rev. B **86**, 081406 (2012).
- 26 [25] K. Y. Y. Han, S. K. Kim, C. Eggeling, and S. W. Hell, *Metastable dark States enable*  
27 *ground state depletion microscopy of nitrogen vacancy centers in diamond with*  
28 *diffraction-unlimited resolution.*, Nano Lett. **10**, 3199 (2010).
- 29 [26] Y. Mita, *Change of absorption spectra in type-Ib diamond with heavy neutron*  
30 *irradiation.*, Phys. Rev. B **53**, 11360 (1996).
- 31 [27] C. Bradac, T. Gaebel, N. Naidoo, M. J. Sellars, J. Twamley, L. J. Brown, A. S. Barnard,  
32 T. Plakhotnik, A. V. Zvyagin, and J. R. Rabeau, *Observation and control of blinking*  
33 *nitrogen-vacancy centres in discrete nanodiamonds.*, Nat. Nanotechnol. **5**, 345 (2010).
- 34 [28] M. V. Hauf, B. Grotz, B. Naydenov, M. Dankerl, S. Pezzagna, J. Meijer, F. Jelezko, J.  
35 Wrachtrup, M. Stutzmann, F. Reinhard, and J. A. Garrido, *Chemical control of the*  
36 *charge state of nitrogen-vacancy centers in diamond*, Phys. Rev. B **83**, 081304 (2011).
- 37 [29] T. W. Shanley, A. A. Martin, I. Aharonovich, and M. Toth, *Localized chemical switching*  
38 *of the charge state of nitrogen-vacancy luminescence centers in diamond*, Appl. Phys.  
39 Lett. **105**, 063103 (2014).
- 40 [30] N. Mizuochi, T. Makino, H. Kato, D. Takeuchi, M. Ogura, H. Okushi, M. Nothaft, P.  
41 Neumann, A. Gali, F. Jelezko, J. Wrachtrup, and S. Yamasaki, *Electrically driven*  
42 *single-photon source at room temperature in diamond*, Nat. Photonics **6**, 299 (2012).
- 43 [31] B. Grotz, M. V. Hauf, M. Dankerl, B. Naydenov, S. Pezzagna, J. Meijer, F. Jelezko, J.  
44 Wrachtrup, M. Stutzmann, F. Reinhard, and J. A. Garrido, *Charge state manipulation*  
45 *of qubits in diamond.*, Nat. Commun. **3**, 729 (2012).
- 46 [32] H. Kato, M. Wolfer, C. Schreyvogel, M. Kunzer, W. Müller-Sebert, H. Obloh, S.  
47 Yamasaki, and C. E. Nebel, *Tunable light emission from nitrogen-vacancy centers in*  
48 *single crystal diamond PIN diodes*, Appl. Phys. Lett. **102**, 151101 (2013).
- 49 [33] M. V. Hauf, P. Simon, N. Aslam, M. Pfender, P. Neumann, S. Pezzagna, J. Meijer, J.  
50 Wrachtrup, M. Stutzmann, F. Reinhard, and J. A. Garrido, *Addressing single nitrogen-*

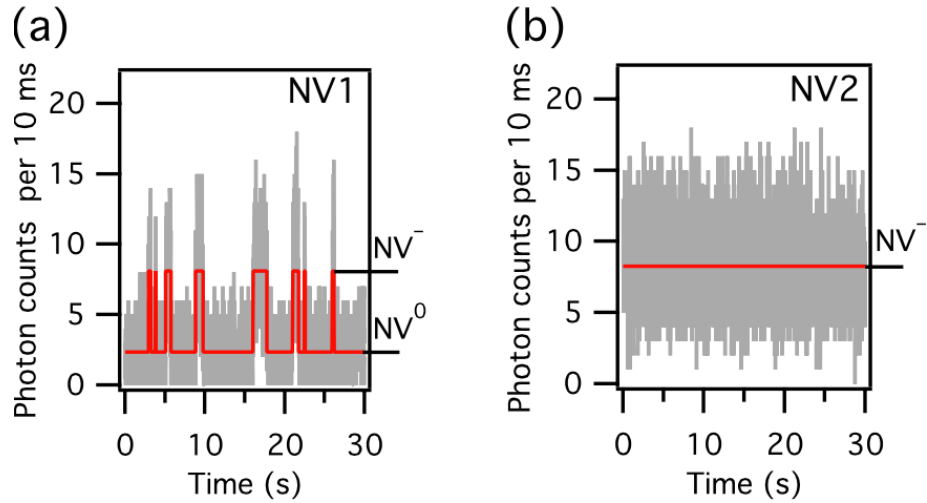
- 1 *vacancy centers in diamond with transparent in-plane gate structures.*, Nano Lett. **14**,  
2 2359 (2014).
- 3 [34] Y. Doi, T. Makino, H. Kato, D. Takeuchi, M. Ogura, H. Okushi, H. Morishita, T.  
4 Tashima, S. Miwa, S. Yamasaki, P. Neumann, J. Wrachtrup, Y. Suzuki, and N.  
5 Mizuochi, *Deterministic Electrical Charge-State Initialization of Single Nitrogen-*  
6 *Vacancy Center in Diamond*, Phys. Rev. X **4**, 011057 (2014).
- 7 [35] J. P. Goss, P. R. Briddon, R. Jones, and S. Sque, *Donor and acceptor states in*  
8 *diamond*, Diam. Relat. Mater. **13**, 684 (2004).
- 9 [36] K. Groot-Berning, N. Raatz, I. Dobrinets, M. Lesik, P. Spinicelli, A. Tallaire, J. Achard,  
10 V. Jacques, J.-F. Roch, A. M. Zaitsev, J. Meijer, and S. Pezzagna, *Passive charge*  
11 *state control of nitrogen-vacancy centres in diamond using phosphorous and boron*  
12 *doping*, Phys. Status Solidi A **211**, 2268 (2014).
- 13 [37] M. Katagiri, J. Isoya, S. Koizumi, and H. Kanda, *Lightly phosphorus-doped*  
14 *homoepitaxial diamond films grown by chemical vapor deposition*, Applied Physics  
15 Letters **85**, 6365 (2004).
- 16 [38] See Suplimental Materials at [URL will be inserted by publisher] for details of the  
17 experiments.
- 18 [39] A. Dréau, M. Lesik, L. Rondin, P. Spinicelli, O. Arcizet, J.-F. Roch, and V. Jacques,  
19 *Avoiding power broadening in optically detected magnetic resonance of single NV*  
20 *defects for enhanced dc magnetic field sensitivity*, Physical Review B **84**, 195204  
21 (2011).
- 22 [40] J. A. van Wyk, E. C. Reynhardt, G. L. High, and I. Kiflawi, *The dependences of ESR*  
23 *line widths and spin-spin relaxation times of single nitrogen defects on the*  
24 *concentration of nitrogen defects in diamond*, J. Phys. D: Appl. Phys. **30**, 1790 (1997).
- 25 [41] N. Mizuochi, H. Watanabe, J. Isoya, H. Okushi, and S. Yamasaki, *Hydrogen-related*  
26 *defects in single crystalline CVD homoepitaxial diamond film studied by EPR*, Diam.  
27 Relat. Mater. **13**, 765 (2004).
- 28 [42] N. Mizuochi, P. Neumann, F. Rempp, J. Beck, V. Jacques, P. Siyushev, K. Nakamura,  
29 D. J. Twitchen, H. Watanabe, S. Yamasaki, F. Jelezko, and J. Wrachtrup, *Coherence*  
30 *of single spins coupled to a nuclear spin bath of varying density*, Phys. Rev. B **80**,  
31 041201 (2009).
- 32
- 33

1  
2 **FIGURES**



3  
4 Figure 1: (a) Donor energy levels of phosphorus (P) and nitrogen (P1) donors and acceptor level  
5 labelled (-/0) of the NV center with respect to conduction-band edge of diamond. (b) PL raster-scan  
6 images of single NV centers in n-type diamond (sample A,  $[P] = 5 \times 10^{16}$  atoms/cm<sup>3</sup>) under 100 μW,  
7 532 nm illumination. Most single NVs show similar optical properties under these illumination  
8 conditions. (c) Same as panel (b) but for 100 μW, 593 nm illumination. Fluorescence count rate of  
9 NV2 is about five times larger than that of NV1.  
10

1



2

3 Figure 2: (a) Time trace of fluorescence of NV1 under continuous  $1 \mu\text{W}$ , 593 nm illumination.

4 Photon bursts occur when the charge state transforms into the  $NV^-$  state. The solid red line shows the

5 most probable fluorescence levels, as obtained by the hidden Markov model. Here the average

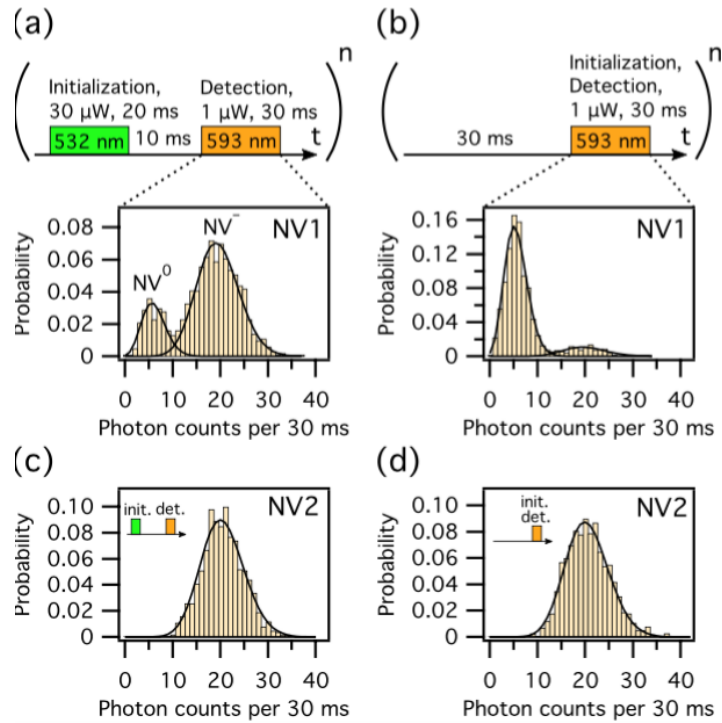
6 lifetimes of the two charge states are 2.92 s ( $NV^0$ ) and 0.59 s ( $NV^-$ ). (b) Time trace of fluorescence

7 of NV2 under the same illumination condition as for NV1. NV2 does not show photon bursts in the

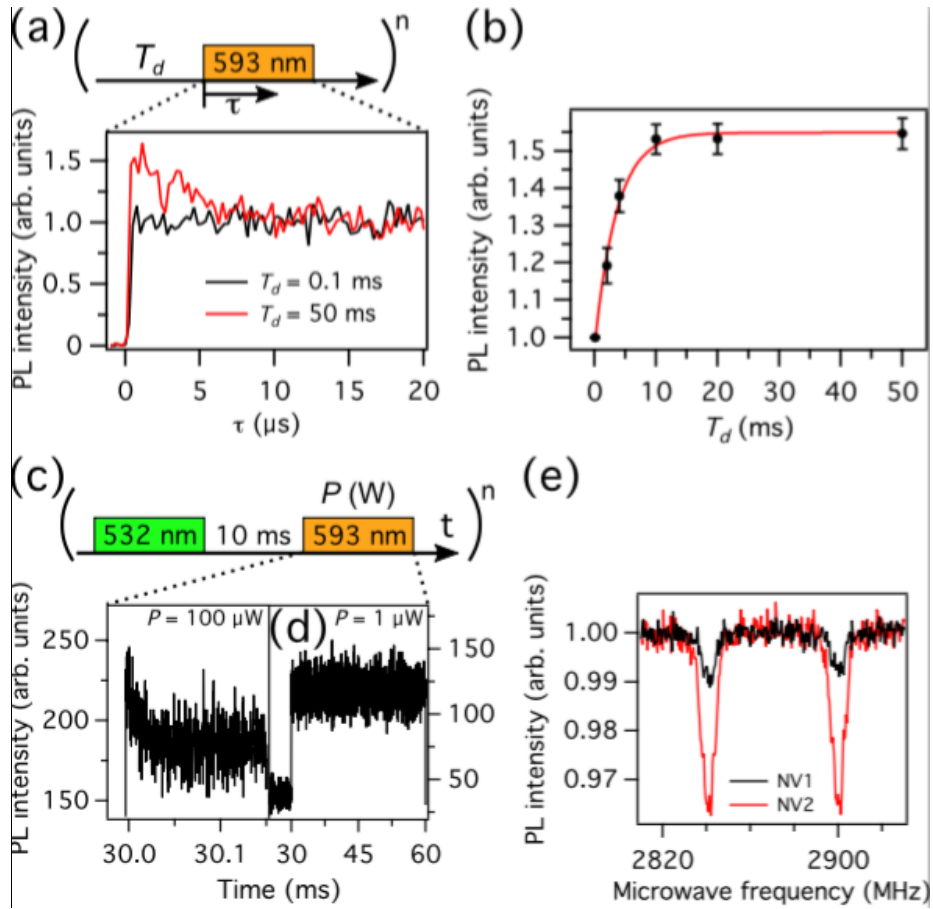
8 trace. A solid red line is the average count rate and is almost the same as the higher counts ( $NV^-$ ) of

9 NV1 in panel (a).

10



1  
 2 Figure 3: Nondestructive single-shot charge-state measurements with two types of charge state  
 3 initialization: (a) 30  $\mu$ W, 532 nm illumination and (b) 1  $\mu$ W, 593 nm illumination. NV1 population  
 4 exhibits a double Poisson distribution that is due to two different charge states. Initialization at 593  
 5 nm drastically decreases the population of the  $NV^-$  charge state. (c), (d) Conversely, NV2 has a  
 6 single peak at the same position as  $NV^-$  irrespective of initialization conditions. We repeated each  
 7 sequence  $n=1000$  times for each histogram.



1  
2 Figure 4: (a) Increase of initial PL intensity of NV2 after time delay  $T_d = 0.1$  and 50 ms under 230  
3  $\mu\text{W}$ , 593 nm illumination. PL intensity of NV2 increases after  $T_d = 50$  ms. We repeated sequence  
4  $n=12,209$  times. (b) PL intensity as a function of  $T_d$ . The fluorescence intensity is normalized to  
5 unity for  $T_d = 0.1$  ms. The solid red line is a fit to a monoexponential with a time constant of 3.55  
6 ms. (c) PL intensity for 593 nm illumination pulse  $T_d = 10$  ms after initialization by 532 nm  
7 illumination pulse. For 100  $\mu\text{W}$  illumination, the PL intensity decays exponentially. (d) Same  
8 measurement as for panel (c) except the illumination was 1  $\mu\text{W}$ , 593 nm. No decay in fluorescence  
9 intensity is observed. We repeated sequence  $n=17,219$  and 9130 for  $P = 100$   $\mu\text{W}$  and 1  $\mu\text{W}$   
10 illumination, respectively. (e) ODMR spectrum of NV1 and NV2 under 200  $\mu\text{W}$ , 593 nm  
11 illumination. Signal intensity from NV<sup>-</sup> of NV2 is almost 4.18 times larger than that from NV1.. The  
12 amplitude of the applied magnetic field was 1 mT along the [111] direction of the diamond crystal.